Int. J. Simul. Multidisci. Des. Optim. **15**, 16 (2024)

https://doi.org/10.1051/smdo/2024013

IJSMDO
Available online at:
https://www.ijsmdo.org

Modelling and Optimization of Complex Systems with Advanced Computational Techniques

REVIEW OPEN ACCESS

Design, analysis and optimization of porous titanium alloys scaffolds by using additive manufacture

Xue Yang[1], Xiujuan Song[2], Guoliang Zhang[3,*], Shubo Xu[1,*], Wenming Wang[4], Kangwei Sun[1], Xiquan Ma[1], Siyu Sun[1], Yuefei Pan[1], Jianing Li[1], Guocheng Ren[1], and Weihai Zhang[5]

[1] Shandong Jianzhu University, School of Materials Science and Engineering, Jinan 250101, China
[2] Jinan Engineering Polytechnic, Jinan 250200, China
[3] Shandong Science and Technology Service Development Promotion Centre, Jinan 250101, China
[4] Shandong Wenling precision forging Technology Co., LTD, Jinan, 271100 Shandong, China
[5] Weifang Fuyuan Supercharger Co., LTD, Weifang, 261206 Shandong, China

Received: 18 April 2024 / Accepted: 25 July 2024

Abstract. In order to have a stronger bond with the surrounding bone, the bone prosthesis needs to have interconnecting pores for bone cells to grow and more importantly to avoid stress shielding. At the same time, human bones have different composition and structure of bone tissue in different parts of the body due to different physical factors of the person, so the elastic modulus of the bones that need to be supported and replaced are not the same. And additive manufacturing has the advantages of rapid, efficient and precise manufacturing of complex shapes and high-quality three-dimensional structures, which can manufacture porous scaffold bone prosthesis, and achieve more accurate mechanical property requirements by controlling the design parameters. To study the effect of design strut length and design strut cross-section diameter size on the elastic modulus of tetrahedral titanium alloy scaffold unit, and with the help of UG NX, several digital models of porous titanium alloy scaffolds were constructed with the strut length and the strut cross-section diameter size as the parameters of variation, and then the elastic modulus of each porous titanium alloy scaffold was measured by ANSYS Workbench 2022, and the elasticity modulus of each porous titanium alloy scaffold was further derived from the relationship between the strut length and strut cross-section diameter size and the porous titanium alloy scaffold. Then the elastic modulus of each porous titanium alloy bracket was measured by ANSYS Workbench 2022, and the mathematical model between the strut length, strut cross-section size and elastic modulus of the porous titanium alloy bracket was further derived. Then, ANSYS Workbench 2022 was used to measure the elastic modulus of each porous titanium alloy bracket and further derive the mathematical model between strut length, strut cross-section diameter size and elastic modulus of the porous titanium alloy bracket, with the help of which the elastic modulus of the porous titanium alloy bracket with specific diameters and strut lengths was finally deduced to validate the correctness of the above predicted mathematical model, and to make reasonable explanations and corrections for the deviations. explanation and correction of deviations. As a result, the rapid prototyping technology can be used to design the required porous titanium alloy bracket in a more detailed way.

Keywords: Additive manufacturing / porous titanium alloy holder / modulus of elasticity numerical calculation

1 Introduction

With the increase of traffic accidents and bone diseases, the problem of human bone defects has become a serious health hazard [1]. Traditional methods of bone defect repair have some drawbacks, so researchers have begun to focus on the application of additive manufacturing (3D printing) technology in the design and analysis of porous titanium alloy scaffolds [2,3]. Issam El Khadiri et al. point out that additive manufacturing or 3D printing has considerable advantages over traditional methods (direct manufacturing, time savings, manufacturing complex geometries, etc.) [4]. Rubén Paz found that the application of porous structures in additively manufactured parts combined with lightweight optimization has a great potential to reduce

* e-mails: sdjz6273@163.com; xsb@sdjzu.edu.cn

weight, production time and cost, combining new methods of computer-aided design and finite element analysis in order to achieve a lightweight parametric optimization of porous structures in additively manufactured parts [5]. Porous titanium alloy scaffolds have good mechanical properties, bio-compatible and corrosion resistance, and are widely used in the field of bone defect repair and bone regeneration [3,6]. Compared with the traditional implantation of solid metal blocks, porous titanium alloy scaffolds mimic the structure and function of natural bone, which is conducive to the growth and repair of tissue cells [6–9]. Metal rapid prototyping technology provides strong support for the preparation of porous titanium alloy scaffolds, and scaffolds with complex structures and shapes can be fabricated by printing metal powder layer by layer [10,11]. In addition, 3D printing offers a wide range of design possibilities that can be interfaced with optimization tools to fully understand the limitations, strengths, and ways to improve additive manufacturing [12].

The elastic modulus is an important parameter in the design and analysis process of porous titanium alloy stents, which can be evaluated by experimental determination or numerical simulation [13,14]. The numerical simulation method predicts the elastic modulus of the stent by building a finite element model [15], which takes into account factors such as stent geometry, material properties and pore structure [13,15–18]. Meanwhile, finite element analysis is also a common method to analyze the mechanical properties of the stent, and the mechanical response of the stent is obtained by solving the mechanical equations and stress balance equations [14]. Arvind Gautam utilized to validate the effectiveness of PE and SME properties of Ni Ti constructed TKA smart tibial portion through Finite Element Analysis (FEA) in ANSYS Workbench [19]. Ji-Hong Zhu used the finite element method to analyze the structural response, and the agreement between numerical simulation and structural experimental results demonstrated the effectiveness of this new structural test method. This new method not only provides quick access to topology-optimized structural design verification, but also significantly reduces structural design turnaround time [20]. The objective of this study is to investigate in depth the mechanical properties of porous titanium alloy stents [21,22], especially the elastic modulus associated with the strut length and strut cross-section diameter [19,20,23,24]. By constructing numerical models, performing finite element analysis and mathematical modeling, the relationship between these parameters and the elastic modulus of the stent can be explored [25–27]. This is of great significance for understanding the application of porous titanium alloy scaffolds in the field of bone defect repair [26,28].

Artificial skeletal scaffold, as an important bone defect repair artificial graft bone material, its internal structural morphology and dimensions have a crucial impact on guiding the regeneration of bones and tissues. The current structural design of artificial skeletal scaffolds still faces problems such as single design level and scaffold performance to be improved. Therefore, in-depth investigation of the shape and structural dimensions of skeletal scaffolds, as well as the influence of porous titanium alloy scaffold parameters, such as rod length, diameter, porosity, etc., on their mechanical and biological properties, and the structural design of scaffolds in combination with the unique advantages of 3D printing technology, aims to provide a solid theoretical foundation for the design of artificial skeletal scaffolds that are more in line with the actual medical needs.

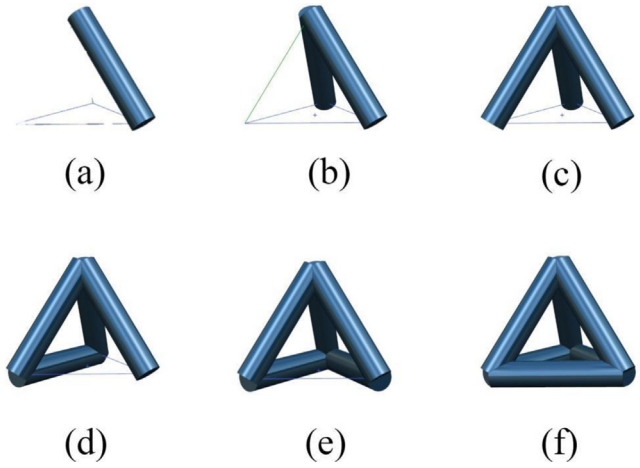

Fig. 1. Design procedure of regular tetrahedron structure unit cell: (a)first step, (b)second step, (c)third step, (d)fourth step, (e) fifth step, (f)sixth step.

Through this study, precise control of the mechanical properties of the scaffolds can be realized to provide patients with more effective bone defect repair solutions and improve their quality of life. With the development of technology, the application of additive manufacturing technology in the field of bone defect repair will be further promoted and applied.

2 Porous titanium scaffold model

2.1 Model design

First of all, in order to construct the porous titanium scaffolds, the unitary body needs to be designed. In this paper, a regular tetrahedron is used as the basic structural unit of the monolithic. Take a cylinder with a length of 2.0 mm and a diameter of 0.4 mm as an example, overlap it with the tetrahedral frame and add the same cylinders gradually until each prong of the tetrahedral frame is covered (six in total), as shown in Figure 1. By doing so, the regular tetrahedral unit with a support rod length of 2.0 mm and a diameter of 0.4 mm is obtained.

After completing the design of the unit cell, the next step is to order the unit cell in 3D space to generate the porous support. First, mark the four center points A, B, C, and D of the bottom surface of the four struts of the unit body. Then, using the transformation function of the UG software, points B and C are selected for transformation operations to obtain a transformed structure b. After a summation operation is performed on the generated geometry, points D and B are selected for transformation to obtain another transformed structure (c). Similarly,

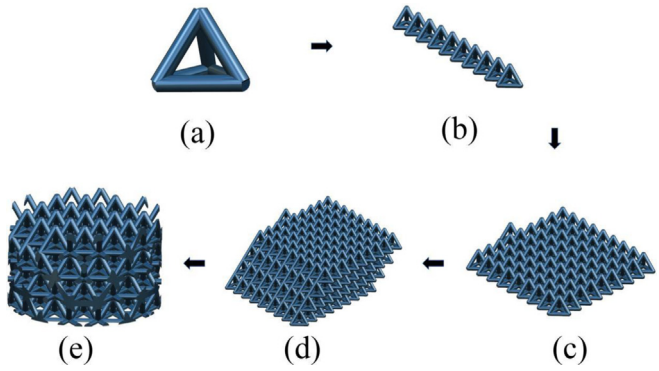

Fig. 2. Design procedure of porous scaffold with regular tetrahedron structure.

after another summation operation is performed on the generated geometry, points D and A are selected for transformation to obtain another transformed structure d. The transformed geometry is then transformed into a structure (c). The transformed structure (d) is then transformed into a structure d. Finally, a cylinder is drawn using the cylinder function by selecting an appropriate position in the x-y plane, and then the cylinder is subjected to summation operation with the generated geometry in Figure 2d to obtain the desired porous stent sample(e).

2.2 Parameter design

The design parameters of regular tetrahedron structured porous stents include the length of the cell stub, the diameter of the stub section, the design porosity and the overall dimensions (diameter, height). In this paper seven different regular tetrahedron structured porous stents are designed which have the same overall dimensions of 10 mm diameter and 7 mm height. Table 1 shows a part of the design parameters of the seven types of stents.

2.3 Comparison of the design of porous scaffolds with different monoliths

Existing studies have shown that in the hexahedral cell, inverted V-60°, inverted V-90°, regular tetrahedron, regular octahedron, and triple-circular intersecting units in the equivalent unit support rod parameters, as shown in Table 2.

Under the same support rod parameters, the orthotetrahedron has the largest compressive strength among the five different types of units, so in order to make the final design of porous titanium bracket with high enough strength and reliability should be selected orthotetrahedron as the basic structural unit of the unit, so the subsequent discussions in this paper are based on the orthotetrahedron unit.

3 Finite element analysis process of porous titanium stents

3.1 Configuration instructions

Creating a geometric model of an object or structure can be accomplished by drawing a digital model of the specimen in UG and importing the model geometry setup port way. A layer of 0.2 mm titanium alloy planar plate was covered above the porous support of the orthotetrahedral structure in Figure 2e to facilitate data logging, presentation of results, and for the convenience of adding boundary conditions, and the effect of this model change on the experimental results was negligible.

In order to make the top of the specimen subjected to uniform pressure, in order to facilitate the recording of the displacement of the top of the loaded model to add the indenter, whose material is rigid (modulus of elasticity than titanium alloy is three orders of magnitude higher), so in the ANSYS Workbench 2022 analysis results of its deformation is very small, can be ignored. The friction coefficient between it and the specimen is set to 0.1 in order to prevent the translation of the rigid body from occurring, and the actual deformation of the specimen has a small effect.

The solver type is set to Direct and a pressure of 10 Gpa is set above the indenter as shown in Figure 3a The pressure support is set at the bottom of the cylindrical specimen of the porous titanium support as shown in Figure 3b.

In order to ensure that the set pressure is within the elastic limit of the porous titanium stent, the pressure applied to the indenter needs to be examined, and in this section, four pressures of 3 MPa, 5 MPa, 7 MPa, and 10 MPa are selected. From the calculated data and experimental analysis, it is known that the top displacement of the specimen has a linear relationship with the magnitude of the pressure, so it can be deduced that the porous titanium bracket is within the elastic limit at a pressure of 10 MPa, and therefore the elastic modulus calculated subsequently is valid.

3.2 Analysis of calculation results

After setting the above configurations, click Solve to solve the results and calculate the modulus of elasticity of the porous titanium scaffold with the formula:

$$\mathrm{Y} = -\frac{\mathrm{p}}{\frac{\Delta x}{\mathrm{h}}} \tag{1}$$

where Δx is the average value of displacement in z-axis direction at the top of the specimen, p is the pressure acting on the indenter at the top of the specimen, and h is the height of the specimen.

$$Y_{L=2.0,d=0.4} = -\frac{10}{\frac{-0.01.3502}{6.7106}} = 4.97\mathrm{GPa} \tag{2}$$

Table 1. Design parameters of a part of the porous titanium alloy stent.

Pole length (mm)	Diameter (mm)	Physical volume (m^3)	Porosity (%)
1.3	0.2	8.89E-08	84.5711524
1.6	0.3	1.22E-07	78.4544514
1.8	0.8	3.99E-07	26.4631189
2.0	0.4	1.29E-07	77.8608099
2.5	0.6	2.03E-07	68.0874059
2.7	1.0	3.67E-07	42.4235644

Table 2. Compressive strength of different unit bodies under the support bar parameters of the same unit body.

No.	Porous stent unit type	Compressive strength σ/MPa
1	Inverted V-60°	53.41 ± 1.60
2	Inverted V-90°	34.00 ± 1.50
3	Regular tetrahedron	71.36 ± 0.45
4	Regular octahedron	42.11 ± 2.84
5	Triple-circula intersecting units	44.39 ± 2.22

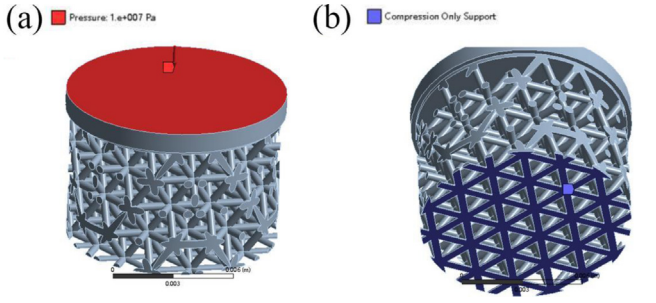

Fig. 3. Compressive strength comparison of five porous scaffolds.

with the example of finite element analysis of a cylindrical specimen of a porous titanium support, the results of the displacement of this specimen at a given pressure can be obtained according to the definition of the modulus of elasticity. Based on the displacement results, the modulus of elasticity of the specimen can be calculated. For example, for a porous titanium bracket specimen with a cell support rod of 2.0 mm in length and 0.4 mm in diameter, the elastic modulus is calculated to be 4.97 GPa under an applied pressure of 10 GPa.

The relationship between porosity and elastic modulus under different support rod lengths can be determined by comparing the elastic modulus data of porous titanium alloy stents corresponding to two groups of the same scale porosity obtained by changing the diameter size of the support rods under two different support rod lengths, fitting the parameters of the function relationship between porosity and elastic modulus of the porous titanium alloy stents under the two lengths with the help of MATLAB and comparing whether the two are the same or not. When the relationship between porosity and elastic modulus is consistent for different brace lengths, the function parameters should be the same for both brace lengths, and vice versa.

In this paper, the differences and similarities of the parameters of the functional relationship between porosity and the elastic modulus of the porous titanium alloy bracket are selected as the basis of judgment for the three cases in which the length of the support rod is 2.0 mm, 2.5 mm and 2.7 mm. The formula for porosity is:

$$P = 100\% \times \left(1 - \frac{v_0}{v}\right). \tag{3}$$

Table 3. MATLAB parameter fitting values for three cases with support rod lengths of 2.0 mm, 2.5 mm and 2.7 mm.

Support rod length (mm)	a	b
2.0	5.3645263538	–2.925548873
2.5	4.8173957000	–3.1775045559
2.7	5.5542815337	–3.121846216

The porosity as a function of the modulus of elasticity of the porous titanium alloy support is given by:

$$Y = a\left(e^{b(p-1)} - 1\right) \tag{4}$$

The parameter values for the three cases of support bar lengths of 2.0 mm, 2.5 mm and 2.7 mm are shown in Table 3.

There are some differences in the parameters, indicating that the consistency of the relationship between porosity and elastic modulus under different support rod lengths is not strictly established, and the elastic modulus-porosity curves of the three can be more intuitively observed through the figure. A more obvious separation of the three curves begins to appear after the porosity is lower than 0.5.

By analyzing Figure 4, it can be found that the direct study of the influence of porosity on the elastic modulus of the porous titanium stent will appear systematic deviation, which is due to the same porosity may be achieved by a variety of different length and diameter of the support rods,

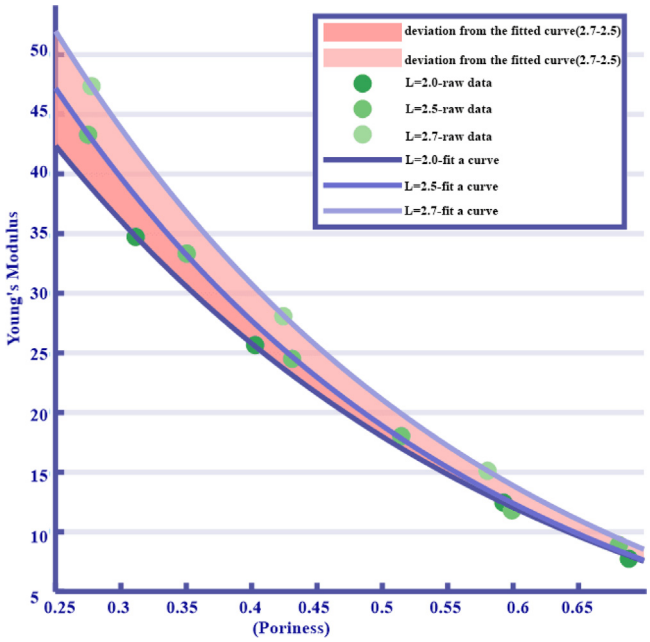

Fig. 4. Modulus of elasticity-porosity curves for three cases with support rod lengths of 2.0 mm, 2.5 mm and 2.7 mm.

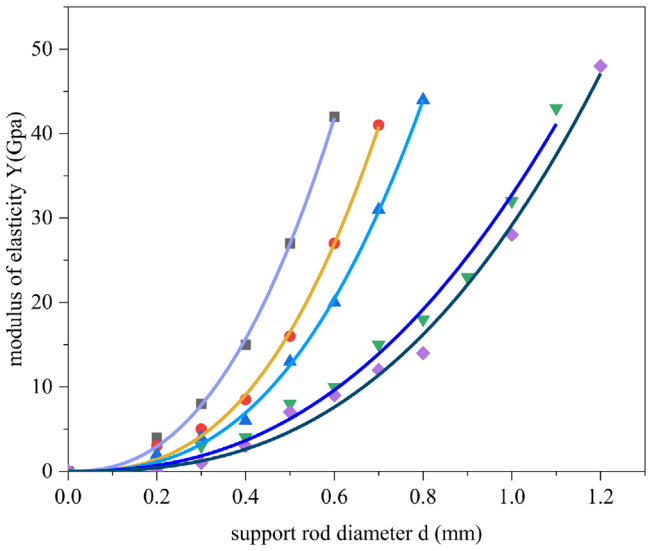

Fig. 5. Fitting curve between the diameter d of the support rod and the elastic modulus Y of the porous titanium support when the length of the support rod L = 1.3 mm, 1.5 mm, 1.8 mm, 2.3 mm, 2.5 mm and 2.7 mm.

which also makes the same porosity may appear in different elastic modulus, so in the subsequent construction of the model in this paper, we will directly on the support rods between the elastic modulus relationship between the length and diameter of the support rods and the porous titanium stent. The relationship between the length and diameter of the support rod and the elastic modulus of the porous titanium support is investigated.

4 Modulus of elasticity model construction

4.1 Modulus of elasticity model construction

First presumed in a certain support rod length under the support rod diameter and porous titanium bracket elastic modulus of the mathematical model, there can be observed in a certain support rod length L under the support rod diameter d and porous titanium bracket elastic modulus Y scatter plot to determine the general trend between. It can be inferred that a certain support rod length L under the support rod diameter d and porous titanium bracket elastic modulus Y is an exponential relationship between the combination of the above analysis to determine the relationship function:

$$Y = f_p(d, L) = p_1\left(e^{p_2 d} - 1\right) \tag{3}$$

with the help of the above analysis, the empirical functional relationship between the support rod diameter d and the elastic modulus Y of the porous titanium support for a certain support rod length L is determined and its feasibility is verified, and then it can be generalized to a wider range. A series of support rod lengths L_1,L_2,L_3..., are set and analyzed above, and the parameters of each function are obtained with the help of MATLAB nonlinear function fitting to get the corresponding functional relationship in Figure 5.

Parameter p_i can be obtained from the above analysis, here in this paper L takes the value with the corresponding function parameter p_i as shown in the following Table 4.

4.2 Model integration scenario analysis

The process described above obtains a set of data for a set of support bar lengths l versus a parameter p. Observe its scatter plot.

From Figure 6 can be found p_1 in different rod lengths in the vicinity of the value of 2 (in addition to the red data points marked in the figure, this is due to the two-parameter fit, MATLAB provides a customized function to fit function lsqcurvefit using random numbers into the iterative algorithm for parameter approximation to determine the parameters, so a parameter is determined after the other parameter change pattern may be different from the other data fitting When the parameter change pattern is different and thus produce a sudden change, this situation can first be roughly determined by a fitting of the general range of one of the parameters, and then fit here (iterative fitting), then the other parameter may show a better regularity, this paper also adopts this method for the fitting parameter processing.) In order to improve the significance of the correlation between p_2 and the length of the support rod as well as to simplify the function, p_1 is set as a constant here, so the public is modified to:

$$Y = f_p(d, L) = 2\left(e^{pd} - 1\right). \tag{4}$$

Here p_2 will be noted as p.

Table 4. MATLAB parameter fitting values for different support rod lengths.

D	1.3 mm	1.6 mm	1.8 mm	2.0 mm	2.3 mm	2.5 mm	2.7 mm
p1	3.16511	1.97036	2.05402	1.95413	3.34651	1.87997	2.01515
p2	4.43914	4.42065	3.93085	3.27342	2.35341	2.90667	2.67198

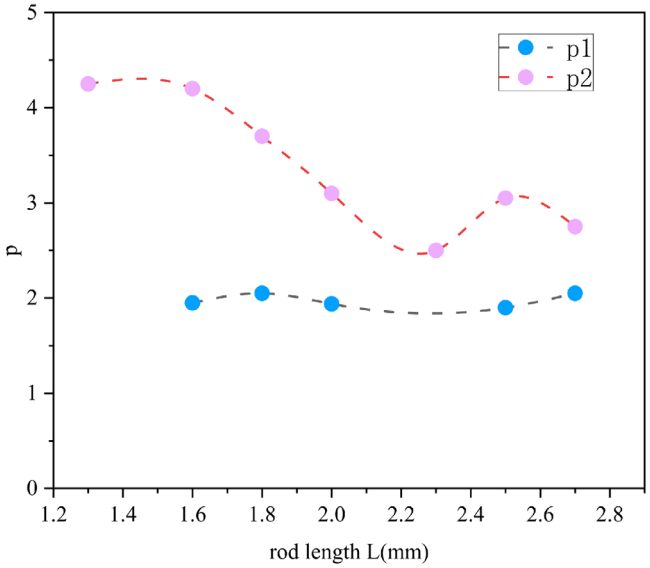

Fig. 6. Scatter diagram of support rod length l and parameter p.

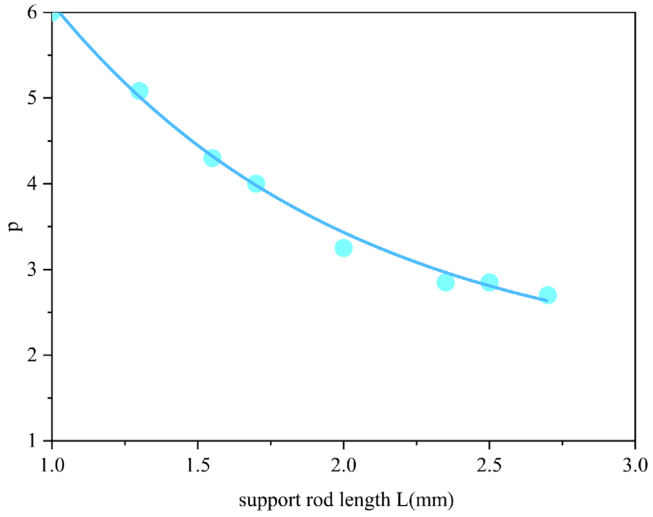

Fig. 7. Fitting curve between the length of the support rod L and the corresponding function parameter.

Next, after re-fitting the parameters of the modified functional equation for the elastic modulus Y of the multi-hollow titanium alloy bracket under a series of support rod lengths L_1,L_2,L_3..., under which the modified functional equation for the modulus of elasticity Y of the multi-hollow titanium alloy bracket under which the diameter d of the support rod is for the modulus of elasticity Y is parametrically fitted, In Figure 7, a new set of support rod lengths L with the corresponding functional parameter p data support rod lengths L with the corresponding functional parameter p data relational equation for the support rod lengths L with the corresponding functional parameter p data is obtained:

$$p = s(\mathrm{l}) = e^{-0.522\mathrm{l}}. \tag{5}$$

4.3 Model program presumptions

With the help of the above analysis, the functional equation of the diameter d and length l of the unit body support rod for the elastic modulus Y of the multi-hollow titanium alloy bracket:

$$\begin{aligned} \mathrm{Y} &= \mathrm{f}(\mathrm{d},\mathrm{l}) = \mathrm{f}_{\mathrm{s(l)}}(\mathrm{h}(\mathrm{d},\mathrm{l})) \\ \mathrm{Y} &= 2\mathrm{e}^{10.0843\mathrm{e}^{-0.522\mathrm{l}}\mathrm{d}}. \end{aligned} \tag{6}$$

The function can be more intuitively demonstrated by its three-dimensional graph to have a high degree of fit to the original data, in Figure 8.

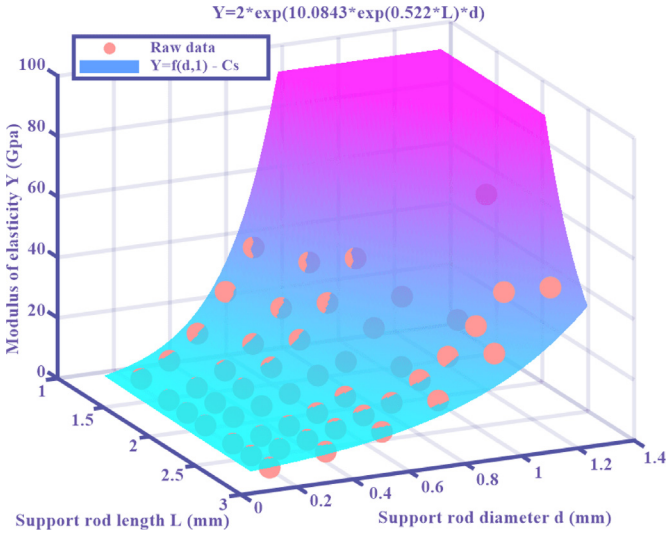

Fig. 8. Comparison between $Y = f(d, l)$ calculation surface and original data.

It should be noted that the applicability of the mathematical model is limited to porosities greater than 30% and that in engineering applications of prosthetic grafts, the function parameter settings can be restricted to higher porosity ranges to improve prediction confidence.

5 Finite element model checking

5.1 Model accuracy tests

Yuchen Ji after comparing the data obtained from the FEA, a noteworthy trend emerges: all the data derived from the FEA exceed the values obtained through testing. This observation is consistent with the initial hypothesis of the experiment – that FEA represents an idealized experiment. The results of the specific experimental study suggest that the degradation of mechanical properties observed in SLM-produced porous titanium alloy ventilators may be related to factors such as non-uniformity of the particle size in the powder, oxidation of the powder and the complexity of the manufacturing process [29]. Overall, finite element analysis can be roughly screened to meet the elastic modulus range of porous skeletal scaffolds with good predictive results, which has far-reaching implications for assessing the mechanical properties of implants as well as minimizing 3D printing consumables.

Jialiang Li, in his study on the structure of Voronoi porous skeletal scaffolds, pointed out that factors such as pore size, porosity and rod diameter affect the performance of the scaffolds. Finite element analysis (FEA) can explain the force transfer and stress distribution in a detailed and intuitive manner and is similar to the subsequent experimental data, which is very predictable and simulative [30].

In summary, it can be clearly recognized that finite element analysis (FEA) exhibits significant value in the study of porous skeletal scaffolds. That is, FEA represents idealized experimental conditions. The prediction is good and has far-reaching significance in evaluating the mechanical properties of implants and reducing 3D printing consumables. Therefore, this study adopts FEA to simulate the design, analysis and optimization of porous titanium alloy skeletal scaffolds, and comprehensively considers its influencing factors to achieve ideal experimental results with high accuracy and implementation.

Next, the reliability of the model constructed in this paper was tested by designing a porous titanium scaffold prosthesis for the human femur as an example. The literature states that the modulus of elasticity of the human femur is 17 GPa, and with the help of the formula, the parameters of the rod length and diameter of the orthotetrahedral unit body were calculated with $L = 2.6$ mm and $d = 0.8244$ mm.

The average value of displacement in z-axis direction at the tip is -0.0038586 mm as measured by ANSYS Workbench, as shown in Figure 9 the pressure applied by the indenter is 10 GPa, and the height of the specimen is 6.7 mm which is brought into the equation:

$$Y_{L=2.0,d=0.4} = -\frac{10}{\frac{-0.0038586}{6.7}} = 17.36\text{GPa}. \quad (7)$$

Its relative error to the calculated value of the mathematical model constructed in this paper is:

$$\eta = \frac{17.36 - 17.00}{17.00} \times 100\% = 2.12\%. \quad (8)$$

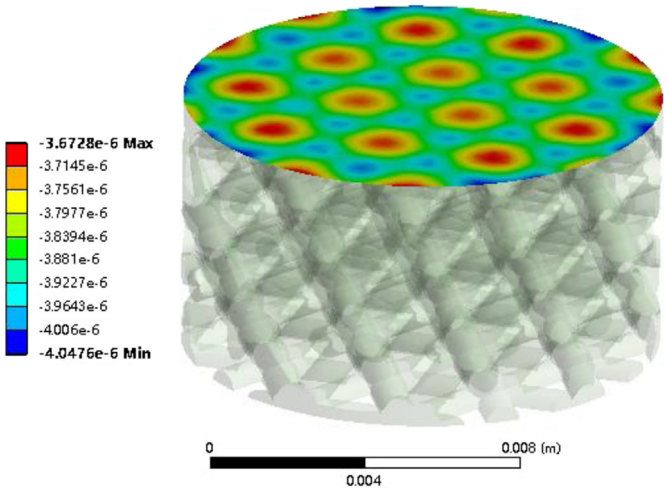

Fig. 9. The unit body support rod length $L = 2.6$ mm, diameter $d = 0.8244$ mm porous titanium support sample top displacement in the z axis direction.

It can be seen that with the help of the mathematical model constructed in this paper to obtain the target modulus of elasticity of the porous titanium alloy stent prosthesis of the unitary support rod length and diameter of the unitary support rod with good reliability, can be customized for a specific bone graft needs specific porous titanium alloy stent prosthesis, to improve the degree of accuracy of its customization, and is also conducive to reducing the customization of the cost.

5.2 Model strength check

Next, the strength reliability of the human femoral porous titanium scaffold prosthesis was examined.

In daily life, the greater force on the femur is when going up and down the stairs, single-legged weight-bearing, the weight-bearing side of the femoral head to withstand more than 3–4 body weight pressure, the model is shown in Figure 10 let a person's body weight is 100 kg, the diameter of the femur is 6 cm, then the pressure on the femur is:

$$\text{p} = \frac{\text{F}}{\text{A}} = \frac{\text{nmg}}{\pi\left(\frac{\text{d}}{2}\right)^2} = \frac{4 \times 100 \times 9.8}{\pi\left(\frac{6}{2}\right)^2} \times 10^4 = 1.39\,\text{MPa}. \quad (9)$$

Therefore, 10 MPa is given to the specimen in the simulation, which can be sufficiently used to check whether the strength requirements for daily life are met.

6 Conclusions

The maximum stress value of the human femoral porous titanium alloy scaffold specimen at 10 MPa was 216.12 MPa, which is less than the compressive yield strength of titanium alloy of 930 MPa, and therefore the human femoral porous titanium alloy scaffold specimen has enough strength to be used in the patient's daily life, as measured by ANSYS Workbench.

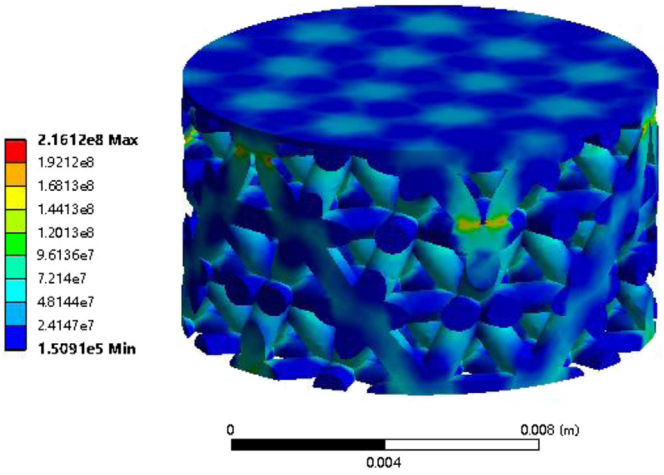

Fig. 10. Overall strain cloud image of porous titanium support specimen with length $L = 2.6$ mm and diameter $d = 0.8244$ mm.

- A model of a porous titanium alloy stent prosthesis for the human femur was successfully designed by the constructed mathematical model and tested for reliability and strength, and the results showed that the stent has good reliability and sufficient strength, which is of positive significance for customizing porous titanium alloy stent prostheses for specific needs and for improving accuracy and reducing costs.
- It is shown that in the case of different units such as hexahedral, inverted V-60°, inverted V-90°, orthotetrahedral, orthoctahedral and tri-circular intersections, having the same support rod parameters, they have different compressive strengths. The orthotetrahedral unit cell has the maximum compressive strength with the same support rod parameters. In order to ensure that the designed porous titanium support has sufficiently high strength reliability, the orthotetrahedron is chosen as the basic structural unit of the unit cell.
- By performing finite element analysis on the cylindrical specimen of the porous titanium support, the modulus of elasticity of the specimen can be calculated. For the porous titanium bracket specimen with a cell support rod length of 2.0 mm and a diameter of 0.4 mm, the calculated modulus of elasticity is 4.97 GPa under an applied pressure of 10 GPa.
- In the accuracy test in the low elastic modulus range, the relative error between the calculated and actual values of the target elastic modulus was obtained to be 2.12%. This indicates that using this mathematical model can provide better access to the unitary support bar parameters of porous titanium stent prostheses with specific modulus of elasticity, thus improving the accuracy and reducing the cost of stent customization.

Acknowledgments

This study was supported by Key R&D Program of Shandong Province (2023TSGC085, 2023TSGC0119, 2023TSGC0759, 2023TSGC0961) and Shandong Province Development and Reform Commission Special Needs Talents Project: R&D and Application of Intelligent Manufacturing Key Technology for High Performance Railway Wheel Unit Production Line.

Declaration of competing interest

The authors declare that they have no known competing financial interests or personal relationships that could have appeared to influence the work reported in this paper.

Data availability

Data will be made available on request.

Credit authorship contribution statement

Xue Yang wrote the manuscript and responsible for the experimental work. Xiujuan Song wrote the manuscript and responsible for the experimental work. Guoliang Zhang and Shubo Xu contributed to data extraction and format correction of the article. Wenming Wang, Kangwei Sun, Xiquan Ma, Siyu Sun, Yuefei Pan, Jianing Li, Guocheng Ren, Weihai Zhang contributed to formal analysis. All the authors read and approved the final manuscript.

References

1. B. Wang, J. Lan, H. Qiao, L. Xie, H. Yang, H. Lin, X. Li, Y. Huang, Porous surface with fusion peptides embedded in strontium titanate nanotubes elevates osteogenic and antibacterial activity of additively manufactured titanium alloy, Colloids Surf. B **113188**, 224 (2023)
2. C. Song, L. Liu, Z. Deng, H. Lei, F. Yuan, Y. Yang, Y. Li, Y. Jiakuo, Research progress on the design and performance of porous titanium alloy bone implants, J. Mater. Res. Technol. **23**, 2626–2641 (2023)
3. L. Zhao, X. Pei, L. Jiang, C. Hu, J. Sun, F. Xing, C. Zhou, Y. Fan, X. Zhang, Bionic design and 3D printing of porous titanium alloy scaffolds for bone tissue repair, Compos. Part B: Eng. **162**, 154–161 (2019)
4. I. El Khadiri, M. Zemzami, N.-Q. Nguyen, M. Abouelmajd, N. Hmina, S. Belhouideg, Topology optimization methods for additive manufacturing: a review, Int. J. Simul. Multidiscip. Des. Optim. **14** (2023). doi: 10.1051/smdo/2023015
5. R. Paz, M.D. Monzón, B. González, E. Pei, G. Winter, F. Ortega, Lightweight parametric optimisation method for cellular structures in additive manufactured parts, Int. J. Simul. Multidiscip. Des. Optim. **7** (2016). doi: 10.1051/smdo/2016009
6. Y.-W. Cui, L. Wang, L.-C. Zhang, Towards load-bearing biomedical titanium-based alloys: From essential requirements to future developments, Progr. Mater. Sci. **144**, 101277 (2024)
7. W. Abd-Elaziem, M.A. Darwish, A. Hamada, W.M. Daoush, Titanium-based alloys and composites for orthopedic implants applications: a comprehensive review, Mater. Des. **112850** (2024)
8. E. Davoodi, H. Montazerian, A.S. Mirhakimi, M. Zhianmanesh, O. Ibhadode, S.I. Shahabad, R. Esmaeilizadeh, E. Sarikhani, S. Toorandaz, S.A. Sarabi, R. Nasiri, Y. Zhu,

J. Kadkhodapour, B. Li, A. Khademhosseini, E. Toyserkani, Additively manufactured metallic biomaterials, Bioactive Mater. **15**, 214–249 (2022)
9. B. Peng, H. Xu, F. Song, P. Wen, Y. Tian, Y. Zheng, Additive manufacturing of porous magnesium alloys for biodegradable orthopedic implants: process, design, and modification, J. Mater. Sci. Technol. **182**, 79–110 (2024)
10. Á. Serrano-Aroca, A. Cano-Vicent, R. Sabater i Serra, M. El-Tanani, A. Aljabali, M.M. Tambuwala, Y.K. Mishra, Scaffolds in the microbial resistant era: Fabrication, materials, properties and tissue engineering applications, Mater. Today Bio. **16**, 79–110 (2022)
11. X. Wang, S. Xu, S. Zhou, W. Xu, M. Leary, P. Choong, M. Qian, M. Brandt, Y.M. Xie, Topological design and additive manufacturing of porous metals for bone scaffolds and orthopaedic implants: a review, Biomaterials **83**, 127–141 (2016)
12. S. Guessasma, W. Zhang, J. Zhu, S. Belhabib, H. Nouri, Challenges of additive manufacturing technologies from an optimisation perspective, Int. J. Simul. Multidiscip. Des. Optim. **6** (2016). doi: 10.1051/smdo/2016001
13. K. Spranger, C. Capelli, G.M. Bosi, S. Schievano, Y. Ventikos, Comparison and calibration of a real-time virtual stenting algorithm using finite element analysis and genetic algorithms, Comput. Methods Appl. Mech. Eng. **293**, 462–480 (2015)
14. S. Tu, N. Morita, T. Fukui, K. Shibanuma, The s-version finite element method for non-linear material problems, Appl. Math. Modell. **126**, 287–309 (2024)
15. P. Mondal, A. Das, A. Wazeer, A. Karmakar, Biomedical porous scaffold fabrication using additive manufacturing technique: porosity, surface roughness and process parameters optimization, Int. J. Lightweight Mater. Manufact. **5**, 384–396 (2022)
16. X. Wang, D. Zhang, H. Peng, J. Yang, Y. Li, J. Xu, Optimize the pore size-pore distribution-pore geometry-porosity of 3D-printed porous tantalum to obtain optimal critical bone defect repair capability, Biomater. Adv. **154**, 213638 (2023)
17. D. Zhao, Y. Huang, Y. Ao, C. Han, Q. Wang, Y. Li, J. Liu, Q. Wei, Z. Zhang, Effect of pore geometry on the fatigue properties and cell affinity of porous titanium scaffolds fabricated by selective laser melting, J. Mech. Behavior Biomed. Mater. **88**, 478–487 (2018)
18. V. Balasubramani, R. Jeganathan, S. Dinesh Kumar, Numerical analysis of porosity effects on mechanical properties for tissue engineering scaffold, Mater. Today: Proc. (2023)
19. A. Gautam, M.A. Callejas, A. Acharyya, S.G. Acharyya, Shape-memory-alloy-based smart knee spacer for total knee arthroplasty: 3D CAD modelling and a computational study, Med. Eng. Phys. **55**, 43–51 (2018)
20. J.-H. Zhu, K.-K. Yang, W.-H. Zhang, Backbone cup – a structure design competition based on topology optimization and 3D printing, Int. J. Simul. Multidiscip. Des. Optim. **7** (2016). doi: 10.1051/smdo/2016004
21. G. He, P. Liu, Q. Tan, Porous titanium materials with entangled wire structure for load-bearing biomedical applications, J. Mech. Behav. Biomed. Mater. **5**, 16–31 (2012)
22. S. Zou, Y. Mu, B. Pan, G. Li, L. Shao, J. Du, Y. Jin, Mechanical and biological properties of enhanced porous scaffolds based on triply periodic minimal surfaces, Mater. Des. **219**, 110803 (2022)
23. M. Rahatuzzaman, M. Mahmud, S. Rahman, M.E. Hoque, Design, fabrication, and characterization of 3D-printed ABS and PLA scaffolds potentially for tissue engineering, Res. Eng. **21**, 101685 (2024)
24. B. Hoddy, N. Ahmed, K. Al-Lamee, N. Bullett, N. Curzen, N.W. Bressloff, Investigating the material modelling of a polymeric bioresorbable scaffold via in-silico and in-vitro testing, J. Mech. Behavior Biomed. Mater. **120**, 104557 (2021)
25. M. Abbaslou, R. Hashemi, E. Etemadi, Novel hybrid 3D-printed auxetic vascular stent based on re-entrant and meta-trichiral unit cells: finite element simulation with experimental verifications, Mater. Today Commun. **35**, 105742 (2023)
26. J.M. Mercado-Colmenero, C. Martin-Doñate, A novel geometric predictive algorithm for assessing compressive elastic modulus in MEX additive processes, based on part nonlinearities and layers stiffness, validated with PETG and PLA materials, Polym. Test. **133**, 108389 (2024)
27. W.T. Nugroho, Y. Dong, A. Pramanik, M. Chithirai Pon Selvan, Z. Zhang, S. Ramakrishna, Additive manufacturing of re-entrant structures: Well-tailored structures, unique properties, modelling approaches and real applications, Add. Manufactur. **78**, 103829 (2023)
28. C. Xu, Z. Liu, X. Chen, Y. Gao, W. Wang, X. Zhuang, H. Zhang, X. Dong, Bone tissue engineering scaffold materials: Fundamentals, advances, and challenges, Chin. Chem. Lett. **35**, 109197 (2024)
29. Y. Ji, H. Zhang, Z. Jiang, D. Liu, Y. Yang, C. Guan, Y. Su, X. Wang, F. Duan, Research on 3D printed titanium alloy scaffold structure induced osteogenesis: mechanics and in vitro testing, Mater. Today Commun. **40** (2024)
30. J. Li, Y. Yang, Z. Sun, K. Peng, K. Liu, P. Xu, J. Li, X. Wei, X. He, Integrated evaluation of biomechanical and biological properties of the biomimetic structural bone scaffold: Biomechanics, simulation analysis, and osteogenesis, Mater. Today Biol. **24** (2024)

Cite this article as: Xue Yang, Xiujuan Song, Guoliang Zhang, Shubo Xu, Wenming Wang, Kangwei Sun, Xiquan Ma, Siyu Sun, Yuefei Pan, Jianing Li, Guocheng Ren, Weihai Zhang, Design, analysis and optimization of porous titanium alloys scaffolds by using additive manufacture, Int. J. Simul. Multidisci. Des. Optim. **15**, 16 (2024)